

# Metabolic flux and robustness analysis of glycerol metabolism in *Klebsiella pneumoniae*

Qingrui Zhang · Hu Teng · Yaqin Sun ·  
Zhilong Xiu · Anping Zeng

Received: 19 May 2007 / Accepted: 2 August 2007 / Published online: 23 August 2007  
© Springer-Verlag 2007

**Abstract** The knowledge of the mechanism of flux distribution will benefit understanding cell physiology and regulation of metabolism. In this study, the measured fluxes obtained under steady-state conditions were used to estimate intracellular fluxes and identify the robustness of branch points of the anaerobic glycerol metabolism in *Klebsiella pneumoniae* for the production of 1,3-propanediol by metabolic flux analysis. The biomass concentration increased as  $\text{NADH}_2/\text{NAD}^+$  decreased at low initial concentration and inversed at high initial glycerol concentration. The flux distribution revealed that the branch points of glycerol and dihydroxyacetonephosphate were rigid to the environmental conditions. However, the pyruvate and acetyl coenzyme A metabolisms gave cells the flexibility to regulate the energy and intermediate fluxes under various environmental conditions. Additionally, it was found that the formation rate of ethanol and the ratio of pyruvate dehydrogenase to pyru-

vate formate lyase appeared visible fluctuations at high glycerol uptake rate.

**Keywords** 1,3-Propanediol · *Klebsiella pneumoniae* · Metabolic flux analysis · Glycerol metabolism · Metabolic network

## Introduction

1,3-Propanediol (1,3-PD) is a valuable chemical in the synthesis of polyesters, polyethers or polyurethanes. Therefore, its microbial production has been paid much attention [1, 2]. The biological production of 1,3-PD from glycerol was demonstrated for several bacterial strains such as *Klebsiella*, *Citrobacters* and *Clostridia*. *K. pneumoniae* was frequently studied for 1,3-PD production due to its high productivity and 1,3-PD yield [3, 4]. However, compared with the competing chemical processes, the microbial production is difficult to obtain a high 1,3-PD concentration in the fermentation broth. The belief, that an improvement on both product concentration and productivity could enable the microbial production of 1,3-PD with the economy required by these competitive markets, has fueled large efforts in this field [4–7].

The knowledge of cell physiology and metabolism regulation is helpful to further improve the process by a metabolic engineering approach on the strain. The metabolic state is controlled by various transcriptional regulators that normally orchestrate appropriate cellular responses to environmental signals. However, the mechanism is not clear enough so far. For example, under anaerobic conditions, the bioconversion of glycerol is mainly attributed to *dha* system, which is composed of four enzymes: glycerol dehydrogenase (GDH), dihydroxyacetone kinase (DHAK),

---

Q. Zhang · H. Teng · Y. Sun · Z. Xiu (✉)  
Department of Bioscience and Biotechnology,  
Dalian University of Technology, Linggong Road 2,  
Dalian 116023, People's Republic of China  
e-mail: zhlxiu@dlut.edu.cn

Q. Zhang  
Department of Chemical Engineering,  
Qingdao University of Science and Technology,  
Zhengzhou Road 53, Qingdao 266042,  
People's Republic of China

A. Zeng  
Institute of Bioprocess and Biosystems Engineering,  
Technical University Hamburg-Harburg, Denickestr. 15,  
21071 Hamburg, Germany

glycerol dehydratase (GDHt) and 1,3-PD oxidoreductase (PDOR) [8–10]. Ahrens et al. [11] has found that GDHt is the rate-limiting enzyme in the glycerol reductive pathway. Tobimatsu et al. [12] and Zeng and Biebl [4] have obtained high-level expression of the genes encoding GDHt and PDOR, but the concentration of 1,3-PD was not improved. Additionally, it was reported that the specific formation rates of all the products originating from pyruvate metabolism showed significant differences under conditions of oscillation and steady state [13]. Therefore, it is necessary to analyze the metabolic mechanism and understand quantitatively those phenomena reported previously.

Metabolic flux distribution, which represents the actual steady state of the cells, was generally used for studying the properties of cellular metabolism [14]. Two types of approaches based on the stoichiometry are generally possible for the quantification of metabolic flux distribution. One of the most outstanding approaches, which needs additional information of mass isotopomers is using isotopic labels to measure metabolic fluxes in vivo.  $^{13}\text{C}$ -labelling technique has been shown to be very powerful and reliable. Several remarkable results have been obtained in this respect [15–17]. Nevertheless, the experimental effort is quite significant, and the mathematical analysis of the resulting data (isotopomer data) is still a very demanding task, because it requires solving a high-dimensional system of nonlinear equations. As an alternative, the other methodology provides a procedure to determine the metabolic fluxes by only using a stoichiometric model; a reduced set of measured fluxes and applying mass balances around intracellular metabolites. It has been proven to be a valuable tool for understanding cell physiology and regulation of metabolism and has been successfully applied to different microorganisms [18–22]. However, to date, no attempt has been made to understand quantitatively the production of 1,3-PD in *K. pneumoniae* by metabolic flux analysis (MFA).

In this work, the measured fluxes obtained under steady-state conditions were used to estimate intracellular fluxes and identify the robustness of branch points of anaerobic glycerol metabolism in *K. pneumoniae* for 1,3-PD production by MFA. The metabolic flux distribution under different conditions was analyzed in detail. The fluxes through reactions located around important branch points of the metabolism were compared, and the rigidity of branch points was emphatically discussed as the environmental conditions varied. Additionally, visible fluctuations of the ethanol formation rate and the ratio of pyruvate dehydrogenase (PDH) to pyruvate formate lyase (PFL) were observed at high-glycerol uptake rates.

## Materials and methods

### Metabolic network of *K. pneumoniae* during 1,3-PD production

Knowledge about the metabolic network of an organism is essential for understanding its physiology and phenotypic behavior. The metabolic network that described the anaerobic metabolic pathway for 1,3-PD production by *K. pneumoniae* was shown schematically in Fig. 1, which was reconstructed from the partly annotated genome sequence as well as from biochemical and physiological literatures [5, 23]. Note that this metabolic network included the membrane transport, intracellular glycolysis pathway, pentose phosphate pathway (PPP), biomass synthetic pathways, product formation pathways and anaerobic reactions. In previous work [5, 24], the biomass synthesis reaction was simplified as a formation directly from glycerol. In this work, the biosynthetic precursors were considered and it was noted that the independent reactions of separate intracellular intermediates for the corresponding biosynthetic precursors were lumped as one reaction equation, and the biomass formula was assumed to be  $\text{CH}_{1.75}\text{O}_{0.5}\text{N}_{0.25}$  (ash content was 5%) [24]. The coefficients of those intermediates and reducing equivalents in the biomass synthesis reaction were obtained from combining cellular elemental composition data with cellular molecular composition data by incorporating carbon balance and generalized degree of reduction balance. The fluxes from phosphoenolpyruvate to oxalacetate (OA) and from pyruvate to OA were lumped into a single flux in order to obtain a nonsingular matrix.

### Metabolic flux model

A metabolic matrix was constructed based on the law of mass conservation and on the pseudo-steady-state hypothesis on the intracellular intermediate metabolites. The mass balance equations for all the metabolites were expressed in matrix form as:

$$Sv = b \quad (1)$$

where  $S$  was the reaction stoichiometric matrix as defined above,  $v$  was a  $n \times 1$  vector of fluxes or specific reaction rates,  $b$  was a  $n \times 1$  vector for consumption and secretion rates of metabolites.

In this work, a determinate model system was adopted and a flux computer program was developed by using Matlab 7.0 (Mathwork Inc., Natick, MA, USA).

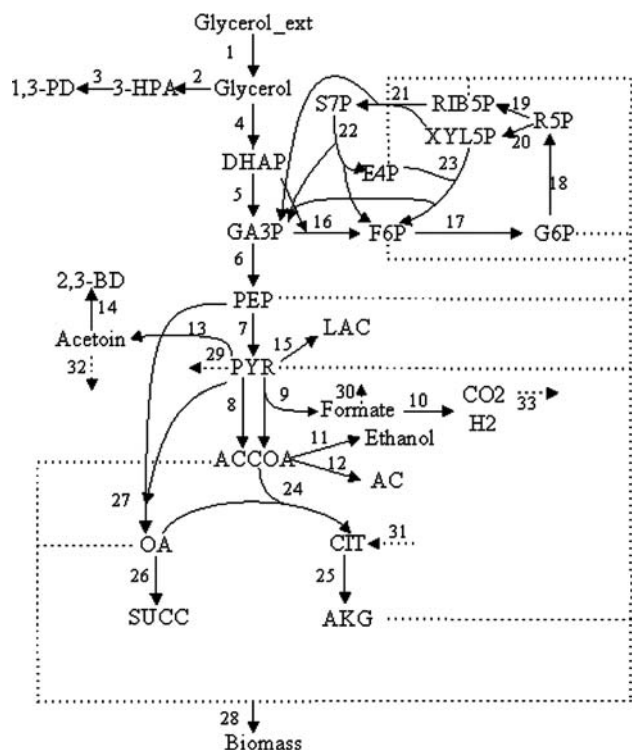


**Fig. 1** Simplified anaerobic pathways of glycerol metabolism and 1,3-PD production in *K. pneumoniae*

Strain, culture conditions, sampling and product analysis

*Klesiella pneumoniae* DSM 2026 obtained from the German Collection of Microorganisms (DSM) was used in this work. Culture medium composition, cultivation conditions, and methods for the determination of fermentation products were reported previously [11, 25, 26].

**Results and discussion**

Metabolic flux distribution

The steady-state experimental data [11, 25] under continuous anaerobic conditions at different dilution rates and initial glycerol concentrations were used in this study. The extracellular specific rates calculated from the experimental data were utilized to obtain the flux distribution using the metabolic network model mentioned above. In Fig. 2, the influences of dilution rates on the flux distributions and fluxes were all normalized by the glycerol uptake rate on a basis of 100. As shown, the flux of 1,3-PD increased from 34.93 to 48.11 as the dilution rate increased from 0.15 to 0.25 h<sup>-1</sup>. The fluxes of ethanol and hydrogen decreased from 32.79 to 20.33, 43.69 to 35.11, respectively, as the dilution rate increased. The results suggested that the formation of

ethanol and hydrogen reduced the 1,3-PD production severely, due to the consumption or no formation of reducing equivalents required for the formation of 1,3-PD. The formation of ethanol was accompanied by the consumption of reducing equivalents. The formation of hydrogen was catalyzed by PFL which did not benefit the formation of reducing equivalents. Therefore, the formation rate of 1,3-PD increased while the formation rate of ethanol and hydrogen decreased as the dilution rate increased. It was also found that other by-products such as 2,3-butandiol, lactate and succinate decreased with the increased dilution rate, but only a little carbon source was used for them. However, the flux of acetate acid (AC) increased slightly from 14.94 to 16.53 as the dilution rate increased. The formation rate of AC had less effect on the production of 1,3-PD.

As shown in Fig. 2, the flux of PFL was much higher than that of PDH, which was consistent with previous experimental results reported by Menzel et al. [27]. The pioneering studies of the group of Guest have found that FNR was a transcription factor in *Escherichia coli* [28]. Its DNA-binding activity was altered upon exposure to stoichiometric levels of oxygen and it was active only during anaerobic growth [29]. Active FNR protein activated and repressed target genes in response to anaerobiosis. It acted as a positive regulator of gene of PFL expressed under anaerobic fermentative conditions [30, 31]. In the previous research, Grabbe et al. [32, 33] has demonstrated the existence of FNR in *K. pneumoniae* and characterized the protein. Therefore, PFL played a dominant role at the pyruvate branch point in glycerol metabolism under

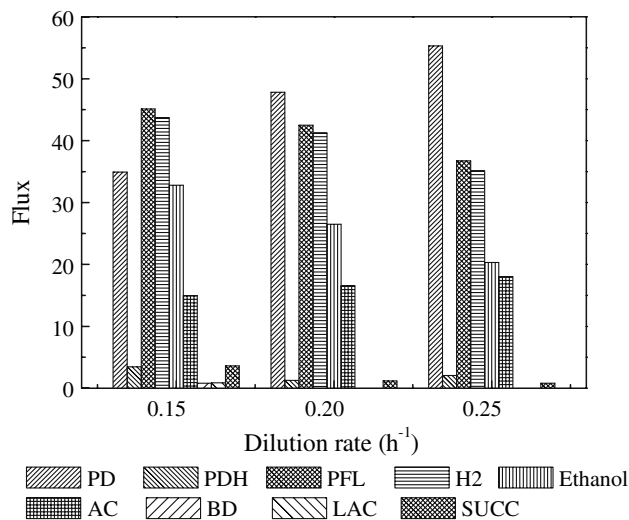


**Fig. 2** Fluxes distribution as a function of the dilution rate. The initial glycerol concentrations are 564, 514 and 523 mmol l<sup>-1</sup> corresponding to the dilution rates of 0.15, 0.2 and 0.25 h<sup>-1</sup>, respectively. Fluxes are normalized by glycerol uptake rate on a basis of 100. Every column represents the flux of PD, PDH, PFL, H<sub>2</sub>, Ethanol, AC, 2,3-BD, LAC, SUCC, respectively from left to right at each dilution rate

anaerobic conditions. However, PDH was an enzyme for oxidatively decarboxylating the pyruvate to acetyl-CoA (ACCOA) and carbon dioxide. This enzymatic reaction produced reduced pyridine nucleotide, which benefited the production of 1,3-PD. So the 1,3-PD concentration might increase if the activity of PDH was improved by changing the regulator of gene expressed.

In Fig. 3, the flux of 1,3-PD increased and then decreased as the initial glycerol concentration increased at a dilution rate of  $0.15 \text{ h}^{-1}$ , exhibiting an optimum initial concentration for the production of 1,3-PD. The formation of hydrogen and ethanol decreased significantly as the initial glycerol concentration increased especially the formation of ethanol almost reach to 0 at a high initial glycerol concentration. However, it was observed that more of other by-products such as 2,3-butanediol and lactate were generated when the glycerol was in excess.

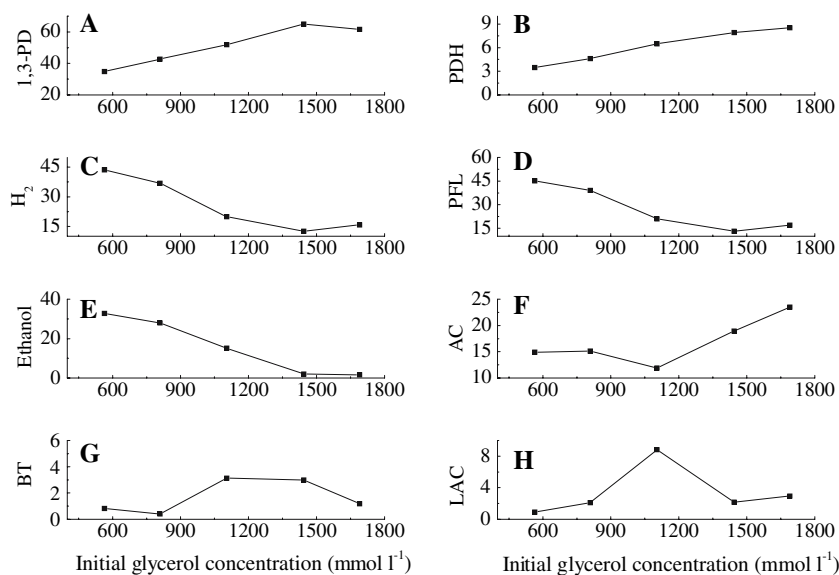
Under excess glycerol conditions, the flux of PDH increased and that of PFL decreased as the initial glycerol concentration increased, which was in accordance with previous report [27]. However, the flux of PFL was much higher than PDH as shown in Fig. 3. This suggested that the activities of PDH and PFL were influenced not only by substrates and end products but also by transcription factors such as above-mentioned FNR. From above mentioned, it was drawn that the yield of 1,3-PD to glycerol was improved as the fluxes of ethanol and PFL decreased or the flux of PDH increased.

Figure 4 showed Effect of initial glycerol concentration on the biomass, the ratio of intracellular  $\text{NADH}_2$  to  $\text{NAD}^+$ , specific rates of ATP and 1,3-PD in *K. pneumoniae* at different dilution rates. It was found that the influence of initial glycerol concentration was independent on dilution rate (Fig. 4a, b). The biomass concentration increased with

initial glycerol concentration at low concentrations and then decreased with initial glycerol concentration at high concentrations (Fig. 4). The ratio of  $\text{NADH}_2$  to  $\text{NAD}^+$  decreased with increasing initial glycerol concentration at low concentration and became relatively constant at high initial glycerol concentration. It was consistent with the previous report [27]. It was reported that the lower  $\text{NADH}_2/\text{NAD}^+$  was benefit for the biomass synthesis [7, 34]. In fact, the glycerol metabolism in *K. pneumoniae* studied by Du was performed at low glycerol concentrations. The only consistent conclusion regarding the effect of pyridine nucleotides from our work and Du seemed to be that a lower ratio of  $\text{NADH}_2$  to  $\text{NAD}^+$  favored the synthesis of biomass at low glycerol concentrations. However, the biomass concentration decreased with the decreasing  $\text{NADH}_2/\text{NAD}^+$  at high glycerol concentrations (Fig. 4). Therefore, it was obtained that the influence of pyridine nucleotides on biomass synthesis changed at different glycerol concentrations.

As depicted in Fig. 4, the specific formation rate of ATP increased smoothly under glycerol-limited conditions and then increased sharply under glycerol excess conditions as the initial glycerol concentration increased. It was consistent with the previous work [35]. This behavior might be attributed to the fact that cells under a higher initial glycerol concentration had an obvious excess of substrate [25]. The rate of ATP production was obviously under excess as well [35]. Therefore, the production rate of energy (ATP) was higher under substrate-sufficient conditions than under substrate-limit conditions. However, glycerol was an inhibitor at its high concentration, the ATP production rate was then decreased as the glycerol concentration reached to a high value (Fig. 4a). In Fig. 4, it was also found that the ATP production rate was coupled with the yield of 1,3-PD to glycerol.

**Fig. 3** Flux distribution as a function of initial glycerol concentration at dilution rate of  $0.15 \text{ h}^{-1}$ . Fluxes are normalized by glycerol uptake rate on a basis of 100. **a** 1,3-PD, **b** PDH, **c**  $\text{H}_2$ , **d** PFL, **e** Ethanol, **f** AC, **g** BT and **h** LAC



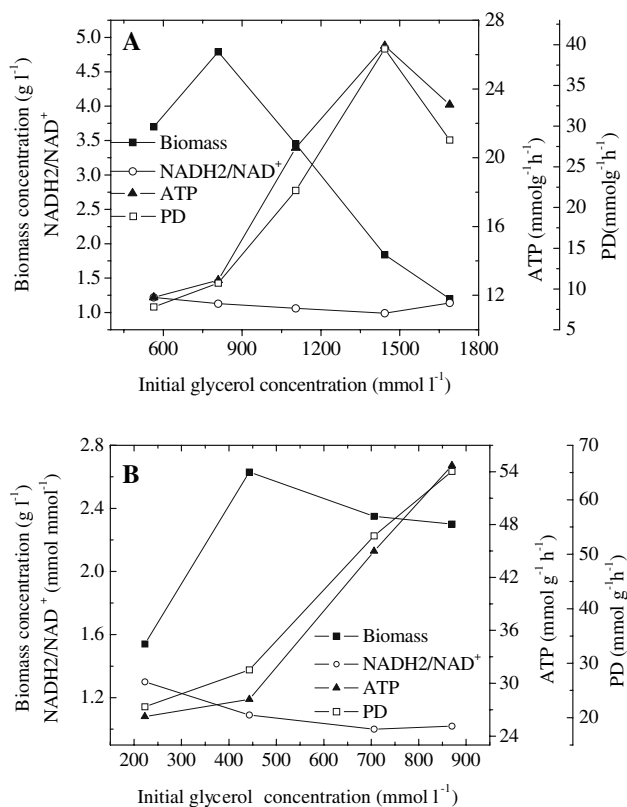


**Fig. 4** Effect of initial glycerol concentration on the biomass, the ratio of intracellular NADH<sub>2</sub> to NAD<sup>+</sup>, specific rates of ATP and 1,3-PD in *K. pneumoniae* at different dilution rates. **a** Dilution rate of 0.15 h<sup>-1</sup>. **b** Dilution rate of 0.35 h<sup>-1</sup>

As shown in Fig. 4, the specific formation rate of 1,3-PD increased and the ratio of NADH<sub>2</sub> to NAD<sup>+</sup> decreased with the initial glycerol concentration. It seemed that a lower NADH<sub>2</sub>/NAD<sup>+</sup> ratio was favorable for the formation of 1,3-PD [27, 34]. However, it contradicted the fact that NADH<sub>2</sub> was a cosubstrate for 1,3-PD formation, and NAD<sup>+</sup> inhibited this reaction [36, 37]. It was reported that the activity of GDH was much higher than that of GDHt and PDOR at lower glycerol concentrations [11]. Therefore, more glycerol channeled into the oxidative pathway and a higher flux of glycolysis was used for biosynthesis, which was accompanied with NADH<sub>2</sub> production at low initial glycerol concentrations. High ethanol formation rates were obtained at low initial glycerol concentrations (Fig. 3e) and the 1,3-PD formation rate was low inversely (Fig. 4). As the glycerol concentration increased, the activity of GDH decreased sharply. Accordingly, the reductive pathway accompanied with the NADH<sub>2</sub> consumption played an important role in glycerol consumption at high glycerol concentrations. The ratio of NADH<sub>2</sub> to NAD<sup>+</sup> decreased as the glycerol concentration increased. It was reported that the 1,3-PD concentration and the ratio of NADH<sub>2</sub> to NAD<sup>+</sup> were all improved through the inactivation of aldehyde dehydrogenase [7]. Therefore, it appeared that the low ratio

of NADH<sub>2</sub> to NAD<sup>+</sup> was not beneficial for the 1,3-PD production.

#### Robustness analysis at branch points

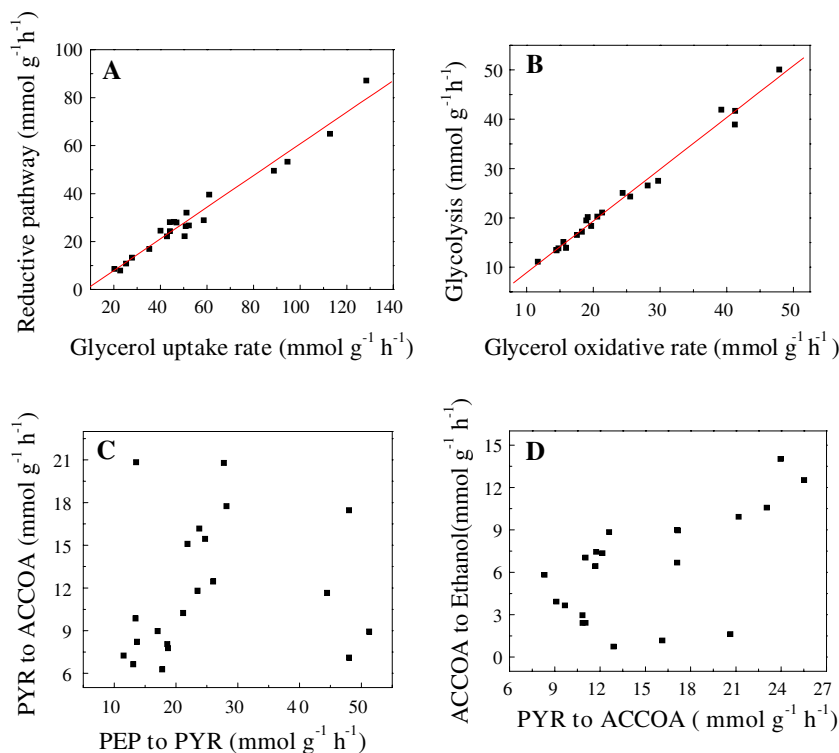
Fluxes generally can respond to altered concentrations of reaction substrate, product or allosteric regulator. To elucidate such kinetic flux control, we estimated absolute fluxes locally at four key branch points as shown in Fig. 5.

As depicted in Fig. 5a, it was seen that the flux distribution was best fitted linearly. The solid line corresponded to the linear fit  $y = -5.30757 + 0.66046x$  with the correlation coefficient of 0.98274, where  $x$  and  $y$  represented the total glycerol uptake rates and the glycerol uptake rates on the reductive pathway, respectively. A linear relation between partitioned fluxes showed a rigid branch point. Therefore, the flux partitioning between glycerol reductive and oxidative pathway was robust against changing environmental conditions. This was consistent with the previous report [11] in which the authors measured the in vitro activities of GDH, GDHt and PDOR and compared them with the corresponding in vivo activities, and it was found that both the in vitro and in vivo activities of the key enzymes varied with nearly the same frequencies during oscillations [11]. Therefore, this rigid control architecture seems to be a built-in feature of the enzymatic kinetics at the glycerol point. The genes for the three enzymes (GDHt, PDOR and GDH) and DHAK were encoded in one regulon named *dha* under anaerobic conditions, and the four enzymes GDHt, PDOR, GDH and DHAK were coordinately expressed [8]. The rigidity of glycerol branch point revealed that it was difficult to improve the concentration of 1,3-PD only through high-level expression of the genes encoding GDHt and PDOR [38].

The second key branch point was dihydroxyacetone-phosphate (DHAP), which could either enter into glycolysis pathway or PPP. Similar to the glycerol branch point, the flux into glycolysis was robust to perturbation and remained largely independent of the oxidative pathway rate (Fig. 5b). It was found that the split between the PPP and the glycolysis pathway varied little as the flux of glycerol oxidative pathway changed. The solid line corresponded to the linear fit  $y = -1.61731 + 1.04918x$  with the correlation coefficient of 0.99772, where  $x$  and  $y$  represented the glycerol flux on oxidative pathway and the glycolysis fluxes, respectively.

The absolute reaction rates and the relative fluxes through alternative pathway such as glycerol and DHAP branch points were shown in Fig. 6 in order to examine whether the environmental conditions affected metabolic state at the level of absolute reaction rates or the relative distribution of fluxes through alternative pathways. It was observed that the relative distribution of fluxes was rather invariant in *K. pneumoniae* that grew on glycerol as the

**Fig. 5** Absolute fluxes at the four key divergent branch points of glycerol catabolism: **a** glycerol. *Solid line* corresponds to linear fit  $y = a + b \times x$ , with  $a = -5.30757$ ,  $b = 0.66046$ . The correlation coefficient  $R$  is 0.98274. **b** DHAP. The flux distribution can be fitted linearly with parameters  $a = -1.61731$ ,  $b = 1.04918$ . The correlation coefficient  $R = 0.99373$ . **c** PYR and **d** Acetyl-coenzyme A (ACCOA)



sole carbon source. The absolute metabolic fluxes in and out of the cell varied by 26–31% around the average value in 90% of all conditions (Fig. 6a, b), whereas relative fluxes varied by only 6–10% (Fig. 6c, d). Therefore, the changing environmental conditions affected absolute fluxes but not their relative distribution. It was noted that the PPP, although an important route for glucose metabolism, appeared to contribute little to the metabolism of glycerol as shown in Fig. 6d. It was due to the fact that PPP pathway was very weak since only a little of the carbon was used for biomass formation in this anaerobic process.

In sharp contrast to the rigid glycerol branch point, flux partitions at pyruvate and acetyl-coenzyme branch points were flexible because none of the outgoing fluxes was correlated with the incoming (Fig. 5c, d). It was concluded that the pyruvate and ACCOA metabolisms gave the cell flexibility to regulate the energy and intermediate fluxes under various environmental conditions. Therefore, the metabolic state was controlled by various transcriptional regulators that normally orchestrate appropriate cellular responses to environmental signals. Although the yield of 1,3-PD could not be improved by over-expressing GDHt and PDOR, the flux distribution could be affected by changing the activity of enzymes around pyruvate and ACCOA branch points. Zhang et al. [7] has improved the 1,3-PD concentration through the inactivation of aldehyde dehydrogenase. It was proposed that the production of 1,3-PD might increase by improving the activity of PDH, which could be changed through the regulator of gene expressed.

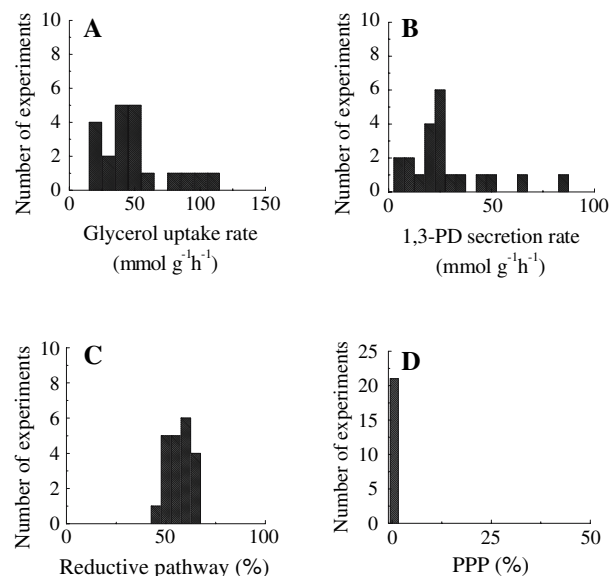


**Fig. 6** Distribution of metabolic fluxes in glycerol conversion by *K. pneumoniae*. **a, b** are absolute fluxes of glycerol uptake and 1,3-PD secretion. **c, d** are relative fluxes of glycerol reductive pathway and PPP pathway, respectively

#### Effect of glycerol uptake rate on the fluxes of other pathways

As shown in Fig. 5, the fluxes of reductive pathway and glycolysis increased as the glycerol uptake rate increased and their relations was linear. The influences of glycerol uptake rate on the other pathways were depicted in Fig. 7.

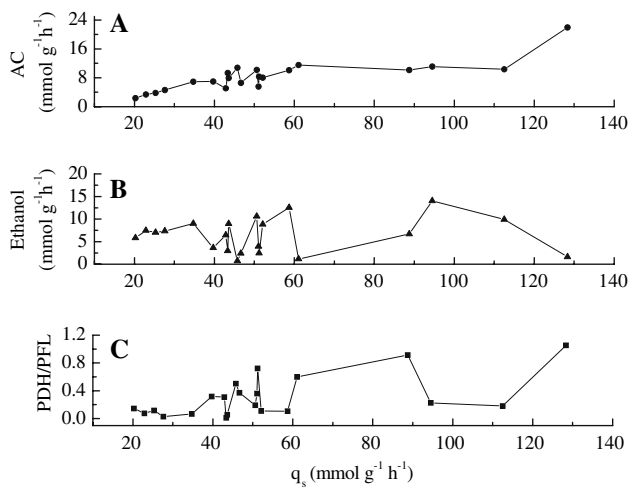


**Fig. 7** The effects of glycerol uptake rates on the fluxes of **a** AC, **b** Ethanol and **c** the ratios of PDH to PFL

Although the branch point of ACCOA was flexible, the formation rate of AC increased as the glycerol uptake rate increased and their correlation was close to linear. The formation rate of ethanol and the ratio of PDH to PFL changed little as the glycerol uptake rate increased at lower glycerol uptake rates. However visible fluctuations were observed as the glycerol uptake rates was more than 40  $\text{mmol g}^{-1} \text{h}^{-1}$ . It was found that increasing glycerol uptake rates could strengthen the oscillation, which amplified amplitude of oscillation. The result was consistent with the previous work that the PFL changed largely during oscillations [27]. This meant that the regulation of the ethanol and PFL flux were sensitive to fluctuations of culture conditions.

## Conclusions

The glycerol metabolism by *K. pneumoniae* was analyzed according to the central metabolic network developed in this work. The flux distribution revealed that the formation rates of ethanol and hydrogen had larger influence on the production of 1,3-PD at lower initial glycerol concentration while the formation rate of ethanol reached to approximate 0 at higher initial glycerol concentrations. The flux distribution showed that the yield of 1,3-PD to glycerol increased as the dilution rate increased at a constant lower initial glycerol concentration. However the yield of 1,3-PD firstly increased and then decreased as the initial glycerol concentration increased at a constant dilution rate. There might exist an optimum initial glycerol concentration at steady states. The ratio of  $\text{NADH}_2$  to  $\text{NAD}^+$  decreased with the initial glycerol concentration. The biomass

concentration increased as the ratio of  $\text{NADH}_2$  to  $\text{NAD}^+$  decreased at low initial glycerol concentrations and inverted at high initial glycerol concentrations.

It was also found that the branch points of glycerol and DHAP were rigid to the environmental conditions and changing environmental conditions often affect absolute fluxes but not their relative distribution. However, the pyruvate and ACCOA metabolisms gave cells flexibility to regulate the energy and intermediate fluxes under various environmental conditions. The flux distribution could be affected by changing the activity of enzymes at pyruvate and ACCOA branch points. Therefore, the 1,3-PD concentration might increase if the activity of PDH was improved by changing the regulator of gene expressed.

**Acknowledgments** This work was supported by the National Natural Science Foundation of China (No. 20576018) and the grant from the Major State Basic Research Development Program of China (973 Program) (No.2007CB714306).

## Appendix 1: List of metabolic reactions

1. Glycerol\_ext  $\rightarrow$  Glycerol
2. Glycerol  $\rightarrow$  3-HPA +  $\text{H}_2\text{O}$
3. 3-HPA +  $\text{NADH}_2$   $\rightarrow$  1,3-PD + NAD
4. Glycerol + NAD + ATP  $\rightarrow$  DHAP +  $\text{NADH}_2$  + ADP
5. DHAP  $\rightarrow$  GA3P
6. GA3P + NAD + PI + ADP  $\rightarrow$  PEP + ATP +  $\text{NADH}_2$  +  $\text{H}_2\text{O}$
7. PEP + ADP  $\rightarrow$  PYR + ATP
8. PYR + COA + NAD  $\rightarrow$  ACCOA +  $\text{CO}_2$  +  $\text{NADH}_2$
9. PYR + COA  $\rightarrow$  ACCOA + Formate
10. Formate  $\rightarrow$   $\text{CO}_2$  +  $\text{H}_2$
11. ACCOA + 2  $\text{NADH}_2$   $\rightarrow$  Ethanol + 2 NAD + COA
12. ACCOA + ADP  $\rightarrow$  AC + ATP + COA
13. 2PYR  $\rightarrow$  Acetoin + 2 $\text{CO}_2$
14. Acetoin +  $\text{NADH}_2$   $\rightarrow$  2,3-BD + NAD
15. PYR +  $\text{NADH}_2$   $\rightarrow$  LAC + NAD
16. GA3P + DHAP + ADP  $\rightarrow$  F6P + ATP
17. F6P  $\rightarrow$  G6P
18. G6P + 2 NADP +  $\text{H}_2\text{O}$   $\rightarrow$  R5P +  $\text{CO}_2$  + 2 NADPH
19. R5P  $\rightarrow$  RIB5P
20. R5P  $\rightarrow$  XYL5P
21. RIB5P + XYL5P  $\rightarrow$  S7P + GA3P
22. S7P + GA3P  $\rightarrow$  E4P + F6P
23. XYL5P + E4P  $\rightarrow$  F6P + GA3P
24. ACCOA + OA  $\rightarrow$  CIT + COA
25. CIT + NAD  $\rightarrow$  AKG +  $\text{NADH}_2$  +  $\text{CO}_2$
26. OA + 2  $\text{NADH}_2$   $\rightarrow$  SUCC + 2 NAD
27. PEP + ADP +  $\text{CO}_2$   $\rightarrow$  OA + ATP
28. 0.35 G6P + 0.523 F6P + 0.952 RIB5P + 0.4075EP + 0.383 PEP + 3.13 PYR + 1.346AKG + 1.6 OA +

- 1.13 ACCOA + 16.3 ATP + 6.75 NAD + 17.8 NADPH → 1g Biomass + 16.3 ADP + 6.75 NADH<sub>2</sub> + 17.8 NADP
29. PYR → PYR\_ext
30. Formate → Formate\_ext
31. CIT\_ext → CIT
32. Acetoin → Acetoin\_ext
33. CO<sub>2</sub> → CO<sub>2</sub>\_ext

## Appendix 2: Summary of abbreviations for the list of metabolic reactions

Table 1

Table 1

Abbreviation	Compound name
2,3-BD	2,3-Butanediol
3-HPA	3-Hydroxypropionaldehyde
AC	Acetic acid
ACCOA	Acetyl-CoA
Acetoin	Acetoin
ADP	Adenosine 5'-diphosphate
AKG	α-Ketoglutarate
ATP	Adenosine triphosphate
CIT	Citrate
CO <sub>2</sub>	Carbon dioxide
DHAP	Dihydroxyacetonephosphate
E4P	Erythrose-4-phosphate
Ethanol	Ethanol
F6P	Fructose 6-phosphate
Formate	Formic acid
G6P	Glucose 6-phosphate
GA3P	Glyceraldehyde 3-phosphate
H <sub>2</sub>	Hydrogen
LAC	Lactate
NADH <sub>2</sub>	Nicotineamide-adeninedinucleotide
NADPH	Nicotineamide-adeninedinucleotide phosphate
OA	Oxaloacetate
PEP	Phosphoenolpyruvate
PI	Inorganic orthophosphate
PYR	Pyruvate
R5P	Ribulose-5-phosphate
RIB5P	Ribose-5-phosphate
S7P	Sedoheptulose-7-P
SUCC	Succinate
XYL5P	Xylulose-5-phosphate

## References

- Biebl H, Menzel K, Zeng AP, Deckwer WD (1999) Microbial production of 1,3-propanediol. *Appl Microbiol Biotechnol* 52:289–297
- Nakamura CE, Whited GM (2003) Metabolic engineering for the microbial production of 1,3-propanediol. *Curr Opin Biotechnol* 14:454–459
- Menzel K, Zeng AP, Deckwer WD (1997) High concentration and productivity of 1,3-propanediol from continuous fermentation of glycerol by *Klebsiella pneumoniae*. *Enzyme Microb Technol* 20:82–86
- Zeng AP, Biebl H (2002) Bulk chemicals from biotechnology: the case of 1,3-propanediol production and the new trends. *Adv Biochem Eng Biotechnol* 74:239–259
- Chen X, Xiu ZL, Wang JF, Zhang DJ, Xu P (2003) Stoichiometric analysis and experimental investigation of glycerol bioconversion to 1,3-propanediol by *Klebsiella pneumoniae* under microaerobic conditions. *Enzyme Microb Technol* 33:386–394
- Cheng KK, Liu DH, Sun Y, Liu WB (2004) 1,3-Propanediol production by *Klebsiella pneumoniae* under different aeration strategies. *Biotechnol Lett* 26:911–915
- Zhang YP, Li Y, Du CY, Liu M, Cao ZA (2006) Inactivation of aldehyde dehydrogenase: a key factor for engineering 1,3-propanediol production by *Klebsiella pneumoniae*. *Metab Eng* 8:578–586
- Forage RG, Lin EC (1982) DHA system mediating aerobic and anaerobic dissimilation of glycerol in *Klebsiella pneumoniae* NCIB 418. *J Bacteriol* 151:591–599
- Tong IT, Liao HH, Cameron DC (1991) 1,3-Propanediol production by *Escherichia coli* expressing genes from the *Klebsiella pneumoniae dha* regulon. *Appl Environ Microbiol* 57:3541–3546
- Sun JB, Heuvel JVD, Soucaille P, Qu YB, Zeng AP (2003) Comparative genomic analysis of *dha* regulon and related genes for anaerobic glycerol metabolism in bacteria. *Biotechnol Prog* 19:263–272
- Ahrens K, Menzel K, Zeng AP, Deckwer WD (1998) Kinetic, dynamic, and pathway studies of glycerol metabolism by *Klebsiella pneumoniae* in anaerobic continuous culture: III. Enzymes and fluxes of glycerol dissimilation and 1,3-propanediol formation. *Biotechnol Bioeng* 59:544–552
- Tobimatsu T, Azuma M, Matsubara H, Takatori H, Niida T, Nishimoto K, Satoh H, Hayashi R, Toraya T (1996) Cloning, sequencing, and high level expression of the genes encoding adenosylcobalamin-dependent glycerol dehydrase of *Klebsiella pneumoniae*. *J Biol Chem* 271:22352–22357
- Zeng AP, Menzel K, Deckwer WD (1996) Kinetic, dynamic, and pathway studies of glycerol metabolism by *Klebsiella pneumoniae* in anaerobic continuous culture: II. Analysis of metabolic rates and pathways under oscillation and steady-state conditions. *Biotechnol Bioeng* 52:561–571
- Fischer E, Sauer U (2005) Large-scale in vivo flux analysis shows rigidity and suboptimal performance of *Bacillus subtilis* metabolism. *Nat Genet* 37:636–640
- Wiechert W, Mollney M, Petersen S, de Graaf AA (2001) A universal framework for 13C metabolic flux analysis. *Metab Eng* 3:265–283
- Zhao J, Shimizu K (2003) Metabolic flux analysis of *Escherichia coli* K12 grown on <sup>13</sup>C-labeled acetate and glucose using GC-MS and powerful flux calculation method. *J Biotechnol* 10:101–117
- Sauer U (2004) High-throughput phenomics: experimental methods for mapping fluxomes. *Curr Opin Biotechnol* 15:58–63
- Stephanopoulos G (1999) Metabolic fluxes and metabolic engineering. *Metab Eng* 1:1–11

19. Shirai T, Nakato A, Izutani N, Nagahisa K, Shioya S, Kimura E, Kawarabayasi Y, Yamagishi A, Gojobori T, Shimizu H (2005) Comparative study of flux redistribution of metabolic pathway in glutamate production by two coryneform bacteria. *Metab Eng* 7:59–69
20. Ozkan P, sariyar B, Utkur FO, Akman U, Hortacsu A (2005) Metabolic flux analysis of recombinant protein overproduction in *Escherichia coli*. *Biochem Eng J* 22:167–195
21. Maczek J, Junne S, Nowak P, Goetz P (2006) Metabolic flux analysis of the sterol pathway in the yeast *Saccharomyces cerevisiae*. *Bioprocess Biosyst Eng* 29:241–252
22. Sanchez AM, Bennett GN, San KY (2006) Batch culture characterization and metabolic flux analysis of succinate-producing *Escherichia coli* strains. *Metab Eng* 8:209–226
23. Sun JB, Zeng AP (2004) IdentiCS—identification of coding sequence and in silico reconstruction of the metabolic network directly from unannotated low-coverage bacterial genome sequence. *BMC Bioinformatics* 5:112–124
24. Zeng AP, Biebl H, Schlieker H, Deckwer WD (1993) Pathway analysis of glycerol fermentation by *Klebsiella pneumoniae*: regulation of reducing equivalent balance and product formation. *Enzyme Microb Technol* 15:770–779
25. Menzel K, Zeng AP, Biebl H, Deckwer WD (1996) Kinetic, dynamic, and pathway studies of glycerol metabolism by *Klebsiella pneumoniae* in anaerobic continuous culture: I. The phenomena and characterization of oscillation and hysteresis. *Biotechnol Bioeng* 52:549–560
26. Menzel K, Zeng AP, Deckwer WD (1997) Enzymatic evidence of involvement of pyruvate dehydrogenase in anaerobic glycerol metabolism by *Klebsiella pneumoniae*. *J Biotechnol* 56:135–142
27. Menzel K, Ahrens K, Zeng AP, Deckwer WD (1998) Kinetic, dynamic, and pathway studies of glycerol metabolism by *Klebsiella pneumoniae* in anaerobic continuous culture: IV. Enzymes and fluxes of pyruvate metabolism. *Biotechnol Bioeng* 60:617–626
28. Guest J, Green J, Irvine A, Spiro S, (1996) The FNR modulon and FNR-regulated gene expression. In: Lin ECC, Lynch AS (eds) Regulation of gene expression in *Escherichia coli*. RG Landes Company, Austin pp 317–342
29. Crack J, Green J, Thomson AJ (2004) Mechanism of oxygen sensing by the bacterial transcription factor fumarate-nitrate reduction (FNR). *J Biol Chem* 279:9278–9286
30. Salmon K, Hung SP, Mekjian K, Baldi P, Hatfield GW, Gunsalus RP (2003) Global gene expression profiling in *Escherichia coli* K12: the effects of oxygen availability and FNR. *J Biol Chem* 278:29837–29855
31. Kang YS, Weber KD, Qiu Y, Kiley PJ, Blattner FR (2005) Genome-wide expression analysis indicates that FNR of *Escherichia coli* k-12 regulates a large number of genes of unknown function. *J Bacteriol* 187:1135–1160
32. Grabbe R, Kuhn A, Schmitz RA (2001) Cloning, sequencing and characterization of Fnr from *Klebsiella pneumoniae*. *Antonie Van Leeuwenhoek* 79:319–326
33. Grabbe R, Klopprogge K, Schmitz RA (2001) FNR Is required for NifL-dependent oxygen control of nif gene expression in *Klebsiella pneumoniae*. *J Bacteriol* 183:1385–1393
34. Du CY, Yan H, Zhang YP, Li Y, Cao ZA (2006) Use of oxidation-reduction potential as an indicator to regulate 1,3-propanediol fermentation by *Klebsiella pneumoniae*. *Appl Microbiol Biotechnol* 69:554–563
35. Zeng AP, Deckwer WD (1995) A kinetic model for substrate and energy consumption of microbial growth under substrate-sufficient conditions. *Biotechnol Prog* 11:71–79
36. Daniel R, Boenigk R, Gottschalk G (1995) Purification of 1,3-propanediol dehydrogenase from *Citrobacter freundii* and cloning, sequencing, and overexpression of the corresponding gene in *Escherichia coli*. *J Bacteriol* 177:2151–2156
37. Barbirato F, Larguier A, Conte T, Astruc S, Bories A (1997) Sensitivity to pH, product inhibition, and inhibition by NAD<sup>+</sup> of 1,3-propanediol dehydrogenase purified from *Enterobacter agglomerans* CNCM 1210. *Arch Microbiol* 168:160–163
38. Menzel K (1999) Analyse der Stoffflüsse und Metabolic Engineering der Glycerinvergaerung zu 1,3-Propandiol durch *Klebsiella pneumoniae*. Ph.D. thesis, German Research Center for Biotechnology (GBF), Braunschweig